3158 *Chem. Mater.* **2010,** *22,* 3158–3164
DOI:10.1021/cm100152q

CHEMISTRY OF MATERIALS
Article

Syntheses of Zinc Oxide and Zinc Hydroxide Single Nanosheets

Ozge Altuntasoglu,*[,†,‡] Yuki Matsuda,[†,‡] Shintaro Ida,[§] and Yasumichi Matsumoto*[,†,‡]

[†]*Graduate School of Science and Technology, Kumamoto University, 2-39-1 Kurokami, Kumamoto 860-8555, Japan,* [‡]*JST, CREST, 5 Sanbancho, Chiyoda-ku, Tokyo 102-0075, Japan, and* [§]*Department of Applied Chemistry, Faculty of Engineering, Kyushu University, 744 Motooka, Nishi-ku, Fukuoka 819-0395, Japan*

Received January 18, 2010. Revised Manuscript Received March 28, 2010

In this study, we present the preparation of zinc oxide (ZnO) and zinc hydroxide ($Zn(OH)_2$) single nanosheets for the first time. ZnO nanosheet was prepared by delamination of layered ZnO film intercalated with the dodecyl sulfate (DS^-) ion which was synthesized by cathodic electrodeposition process. In this case, the addition of La^{3+} ion into the electrolyte was very critical for the further delamination process. On the other hand, $Zn(OH)_2$ nanosheet was prepared by delamination of layered $Zn(OH)_2$ intercalated with the DS^- ion that was prepared by a soft solution process using hexamethylenetetramine (HMT). The thicknesses of the ZnO and $Zn(OH)_2$ nanosheets were about 0.7 and 1.0 nm, respectively. The structures of the nanosheets were discussed with the results of transmission electron microscopy (TEM) and selected area electron diffraction (SAED) images.

Introduction

Exfoliation is the process to delaminate the layered oxide and layered hydroxide materials to get two-dimensional structures called nanosheets having approximate thicknesses of 1 nm and widths of 1 μm. Because nanosheets have intriguing chemical properties used in electrochemical,[1−3] photoelectrochemical,[4−6] and photoluminescent[7−10] applications, delamination of host layers into individual layers has been widely studied. They are used as building blocks to architect hybrid films grown with layer-by-layer self-assembly,[11−13] and Langmuir−Blodgett[14−16] techniques.

ZnO is a piezoelectric and semiconducting material having wide band gap of 3.37 eV and potential applications used in nanoscale dye-sensitized solar cells,[17,18] optoelectronics,[19,20] gas sensors,[21,22] and electronics.[23,24] Recently lamellar ZnO structures have been prepared by sandwiching with organic surfactants by electrodeposition processes.[25−29] It is an easier method for the synthesis of surfactant intercalated ZnO hybrid films rather than synthetic methods. It can be carried out at low temperatures and controlled easily changing several parameters such as deposition time, electrical potential, synthesis temperature, and concentrations of the starting materials.

Up to now, the hybrids composed of ZnO-surfactant films have been of interest to research of synthesis parameters and functionality of these hybrids. Our study,

*Corresponding authors. E-mail: 082d9101@gsst.stud.kumamoto-u.ac.jp (O.A.); yasumi@gpo.kumamoto-u.ac.jp (Y.M.).

(1) Ida, S.; Shiga, D.; Koinuma, M.; Matsumoto, Y. *J. Am. Chem. Soc.* **2008**, *130*, 14038.
(2) Altuntasoglu, O.; Unal, U.; Ida, S.; Goto, M.; Matsumoto, Y. *J. Solid State Chem.* **2008**, *181*, 3257.
(3) Wang, L.; Sakai, N.; Ebina, Y.; Takada, K.; Sasaki, T. *Chem. Mater.* **2005**, *17*, 1352.
(4) Ida, S.; Ogata, C.; Shiga, D.; Izawa, K.; Ikeue, K.; Matsumoto, Y. *Angew. Chem., Int. Ed.* **2008**, *47*, 2480.
(5) Izawa, K.; Yamada, T.; Unal, U.; Ida, S.; Altuntasoglu, O.; Koinuma, M.; Matsumoto, Y. *J. Phys. Chem. B.* **2006**, *110*, 4645.
(6) Sakai, N.; Ebina, Y.; Takada, K.; Sasaki, T. *J. Am. Chem. Soc.* **2004**, *126*, 5851.
(7) Ozawa, T. C.; Fukuda, K.; Akatsuka, K.; Ebina, Y.; Kurashima, K.; Sasaki, T. *J. Phys. Chem. C.* **2009**, *113*, 8735.
(8) Ozawa, T. C.; Fukuda, K.; Akatsuka, K.; Ebina, Y.; Sasaki, T. *Chem. Mater.* **2007**, *19*, 6575.
(9) Ida, S.; Ogata, C.; Unal, U.; Izawa, K.; Inoue, T.; Altuntasoglu, O.; Matsumoto, Y. *J. Am. Chem. Soc.* **2007**, *129*, 8956.
(10) Ida, S.; Ogata, C.; Inoue, T.; Izawa, K.; Unal, U.; Altuntasoglu, O.; Matsumoto, Y. *Chem. Lett.* **2007**, *36*, 158.
(11) Kameyama, T.; Okazaki, K.; Takagi, K.; Torimoto, T. *Phys. Chem. Chem. Phys.* **2009**, *11*, 5369.
(12) Matsuda, A.; Kambayashi, T.; Daiko, Y.; Muto, H.; Sakai, M. J. Eur. Ceram. Soc. **2009**, in press.
(13) Zheng, H.; Tang, F.; Jia, Y.; Wang, L.; Chen, Y.; Lim, M.; Zhang, L.; (Max) Lu, G. *Carbon* **2009**, *47*, 1534.
(14) Tetsuka, H.; Takashima, H.; Ikegami, K.; Nanjo, H.; Ebina, T.; Mizukami, F. *Chem. Mater.* **2009**, *21*, 21.
(15) Akatsuka, K.; Haga, M.-A.; Ebina, Y.; Osada, M.; Fukuda, K.; Sasaki, T. *ACS Nano* **2009**, *3*, 1097.
(16) Yamamoto, T.; Saso, N.; Umemura, Y.; Einaga, Y. *J. Am. Chem. Soc.* **2009**, *131*, 13196.
(17) Zhang, Q.; Chou, T. P.; Russo, B.; Jenekhe, S. A.; Cao, G. *Angew. Chem., Int. Ed.* **2008**, *47*, 2402.
(18) Baxter, J. B.; Walker, A. M.; van Ommering, K.; Aydil, E. S. *Nanotechnology* **2006**, *17*, S304.
(19) Xiang, B.; Wang, P.; Zhang, X.; Dayeh, S. A.; Aplin, D. P. R.; Soci, C.; Yu, D.; Wang, D. *Nano Lett.* **2007**, *7*, 323.
(20) Wang, Z. L. *ACS Nano* **2008**, *2*, 1987.
(21) Wan, Q.; Li, Q. H.; Chen, Y. J.; Wang, T. H.; He, X. L.; Li, J. P.; Lin, C. L. *Appl. Phys. Lett.* **2004**, *84*, 3654.
(22) Li, C. C.; Du, Z. F.; Li, L. M.; Yu, H. C.; Wan, Q.; Wang, T. H. *Appl. Phys. Lett.* **2007**, *91*, 032101.
(23) Lin, Y.-F.; Jian, W.-B. *Nano Lett.* **2008**, *8*, 3146.
(24) Zhou, J.; Fei, P.; Gao, Y.; Gu, Y.; Liu, J.; Bao, G.; Wang, Z. L. *Nano Lett.* **2008**, *8*, 2725.
(25) Gan, X.; Gao, X.; Qiu, J.; Li, X. *Appl. Surf. Sci.* **2008**, *254*, 3839.
(26) Tan, Y.; Steinmiller, E. M. P.; Choi, K.-S. *Langmuir* **2005**, *21*, 9618.
(27) Jing, H. Y.; Li, X. L.; Lu, Y.; Mai, Z. H.; Li, M. *J. Phys. Chem. B.* **2005**, *109*, 2881.
(28) Wang, Y.; Zhang, S.; Wu, X. *Eur. J. Inorg. Chem.* **2005**, 727.
(29) Choi, K.-S.; Lichtenegger, H. C.; Stucky, G. D.; McFarland, E. W. *J. Am. Chem. Soc.* **2002**, *124*, 12402.

 Published on Web 04/19/2010

which is strategically different from the previous ones, has a goal of the fabrication of ZnO nanosheets derived from such hybrid films. Eventually, hybrid films are used from a different perspective, namely as nanosheets' precursors. Since nanosheets contain the functionality of bulk and molecular phases, ZnO single nanosheets having almost 0.7 nm thickness are promising materials for the applications of transparent conduction films, photoelectrochemical studies, and photoluminescence approaches.

In addition to synthesis of ZnO nanosheets, we synthesized single $Zn(OH)_2$ nanosheets derived from layered $Zn(OH)_2$. Layered $Zn(OH)_2$ intercalated with DS^- ions as precursors of $Zn(OH)_2$ nanosheets were prepared by precipitation of aqueous solution of zinc and sodium dodecyl sulfate (SDS) due to the hydrolysis of HMT. This method providing direct intercalation of DS^- ions without any further DS^- ion exchange was developed in our laboratory for the synthesis of layered nickel hydroxides.[1]

Layered $Zn(OH)_2$ is a brucitelike structure and in the same group with the layered double hydroxides which have the general formula of $[M^{2+}_{1-x}M^{3+}_x(OH)_2][A^{n-}_{x/n}\cdot mH_2O]$, where A is an n-valent interlayer guest anion and M^{2+} and M^{3+} are divalent and trivalent metal cations, respectively.[30] The positive charge of the layer is generated by the replacement of divalent metal cation of the brucitelike layer with a trivalent cation and compensated by the interlayer anions. Similarly, layered $Zn(OH)_2$ is a layered metal hydroxide salt having the formula of $M(OH)_{2-x}A^{n-}_{x/n}\cdot mH_2O$.[31] In this structure, the replacement of hydroxyls (OH^-) of the host layer takes place with interlayer anions. We prefer to use SDS to enlarge the interlayer distance which makes it easier to take host layers apart during the delamination. The synthesis of layered zinc hydroxides intercalated with DS^- ions $[Zn(OH)_{2-x}DS^{n-}_{x/n}\cdot mH_2O]$ using hydrolyzing agent of HMT was carried out by soft chemistry route for the first time.

To our best knowledge, this is the first report to synthesize ZnO and $Zn(OH)_2$ single nanosheets. The electrodeposition process enabled us to synthesize the precursors of ZnO nanosheets. We also suggest a structure model for ZnO nanosheets. Consequently, comparison between ZnO and $Zn(OH)_2$ nanosheet preparation and characterization, as well as layered structures of those nanosheets are demonstrated.

Experimental Section

Electrodeposition of Layered ZnO Film. Prior to deposition, indium tin oxide (ITO) coated glass substrates were cleaned ultrasonically in Sibata cleaner (20 wt %), acetone, ethanol, and decarbonated Mili-Q water for 20 min. The cathodic electrodeposition process was performed at −1.1 V vs Ag/AgCl reference electrode for 1 h at 70 °C in an aqueous solution of 0.05 M $Zn(NO_3)_2\cdot 6H_2O$, 0.005 M SDS, and 0.0005 M $La(NO_3)_3\cdot 6H_2O$. ITO coated glass and platinum plates were used as working and counter electrodes, respectively. The deposited samples were washed with a substantial amount of double distilled water and dried overnight. The procedure was repeated several times to get 10 mg layered ZnO film intercalated with DS^- ions.

Soft Solution Synthesis of Layered $Zn(OH)_2$. The layered $Zn(OH)_2$ was synthesized by hydrolyzing of hexamethylenetetramine (HMT). A 0.002 mol portion of $Zn(NO_3)_2\cdot 6H_2O$, 0.005 mol SDS, and 0.012 mol HMT were dissolved in 100 mL double distilled water. The starting pH of the solution was adjusted to 7 by addition of 1 M HCl. The resulting slurry was aged at 90 °C for 1 day. The final precipitate was centrifuged, washed with double distilled water and ethanol, and dried in vacuum for 1 day.

Exfoliation of Layered ZnO Film and Layered $Zn(OH)_2$. A 10 mg portion of layered ZnO film and 5 mg layered $Zn(OH)_2$ were mixed with 20 mL butanol and 20 mL formamide, respectively, for 3 days at room temperature without agitation. Both supernatant solutions were taken as exfoliation solution after centrifuging the solution at 2000 rpm for 20 min to get rid of unexfoliated compounds.

Characterization. The crystal structure of the powders was analyzed using X-ray diffraction (XRD) patterns (Cu Kα radiation, Rigaku RINT-2500VHF). The surface morphology was observed by scanning electron microscopy (SEM, JEOL). The compositions of powders were analyzed with thermogravimetric/differential thermal analysis (TG-DTA, Seiko) following X-ray photoelectron spectroscopy (XPS, VG Scientific Σ-probe). Infrared spectra of the powders were obtained by Fourier-transform infrared spectrometer (FTIR, Perkin-Elmer). The UV−vis absorption spectrum of the layered ZnO film was measured using a UV−vis spectrometer (Jasco-V-550). Emission spectrum was measured using a Jasco FP-6500 spectrofluorometer with a 150 W Xe lamp at room temperature. Atomic force microscopy (AFM, Nanoscope V Digital Instruments) was used to observe the thickness of the nanosheets. Transmission electron microscopy (TEM) images and selected area electron diffraction (SAED) images of powders and nanosheets were recorded at 200 kV using JEM 2000 FX Transmission Electron Microscope. The nanosheet solutions and powders dispersed in ethanol by ultrasonication were dropped onto carbon-coated copper grids, and then, the grids were dried in vacuum at 40 °C for 3 days.

Results and Discussion

Layered ZnO film intercalated with DS^- ions has been self-assembled at the working electrode by cathodic electrodeposition. In this process, reduction of nitrate ions forms OH^- in which pH increases so the deposition of layered ZnO film occurred. Due to the electrostatic interaction between ZnO and DS^- ion, the lamellar hybrid film can be obtained.[29] In the present soft solution route of the layered $Zn(OH)_2$, increase in the temperature promotes the decomposition of HMT and release of NH_3, results alkaline media, and precipitation of Zn^{2+} together with DS^- gives layered $Zn(OH)_2$ intercalated with DS^- ions, according to the our previous study.[1]

Figure 1 depicts the XRD data of layered ZnO film and layered $Zn(OH)_2$ intercalated with DS^- ions. Both of them had (00n) Bragg reflections attributed to the lamellar structures. Layered $Zn(OH)_2$ having eighth order of the (001) diffraction had a better crystallization than

(30) Miyata, S. *Clays Clay Miner.* **1975**, *23*, 369.
(31) Miao, J.; Xue, M.; Itoh, H.; Feng, Q. *J. Mater. Chem.* **2006**, *16*, 474.

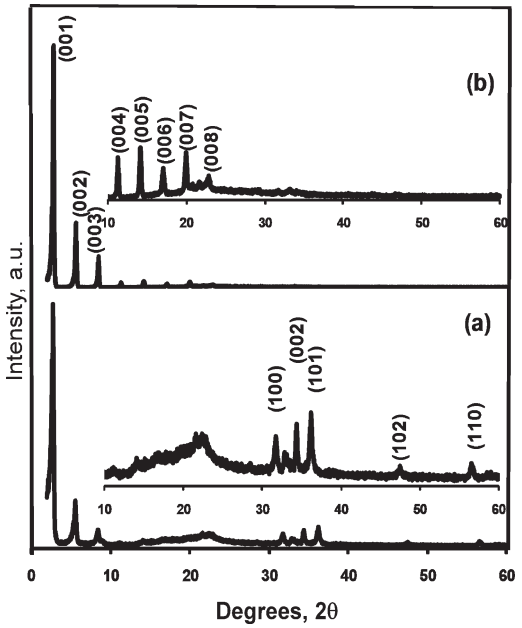

Figure 1. XRD patterns of (a) layered ZnO film and (b) layered $Zn(OH)_2$.

layered ZnO film having weak Bragg reflections of third order of the (001) diffraction. Both the basal spacings of layered ZnO film and layered $Zn(OH)_2$ were calculated to almost 32 Å from the first diffraction peak. The large basal spacing for both samples might be attributed to the bilayer arrangement of DS^- ions in the interlayer domain.[32] The reflections after the 30°(2θ) is due to the presence of the small amount of ZnO particles with wurtzite structure.

In previous approaches, the effect of the surfactans, cosolvents, and cosurfactants types on the layered ZnO film was examined.[26] The structure and morphology of layered film were controlled by changing these parameters. Moreover, addition of metal ion might be another key parameter on the electrodeposited layered ZnO film. In the literature, the effect of lanthanum (La^{3+}) ion on electrodeposition of some metal oxides such as manganese oxides,[33,34] cobalt oxides,[33,34] and nickel oxides[35] existed. The suppression of the growth of metal oxides due to the incorporation into the electrodeposition was observed.[34] Thus, the presence of La^{3+} ion in the starting solution was also investigated.

Figure 2a shows the SEM image of the layered ZnO film prepared in the absence of La^{3+} ion. Although the XRD pattern of the sample (not shown) was similar to the layered ZnO film deposited in the presence of La^{3+} ion, the morphology of film which was aggregated structures was different with the compounds shown in Figure 2b. The aggregate morphology changed to a platelike film when the La^{3+} ion were in the electrolyte solution.

(32) Liang, C.; Shimizu, Y.; Masuda, M.; Sasaki, T.; Koshizaki, N. *Chem. Mater.* **2004**, *16*, 963.
(33) Matsumoto, Y.; Ohmura, H.; Goto, T. *J. Electroanal. Chem.* **1995**, *399*, 91.
(34) Sasaki, T.; Matsumoto, Y.; Hombo, J.; Nagata, M. *J. Electroanal. Chem.* **1994**, *371*, 241.
(35) Matsumoto, Y.; Sasaki, T.; Hombo, J. *J. Electrochim. Acta.* **1993**, *38*, 1145.

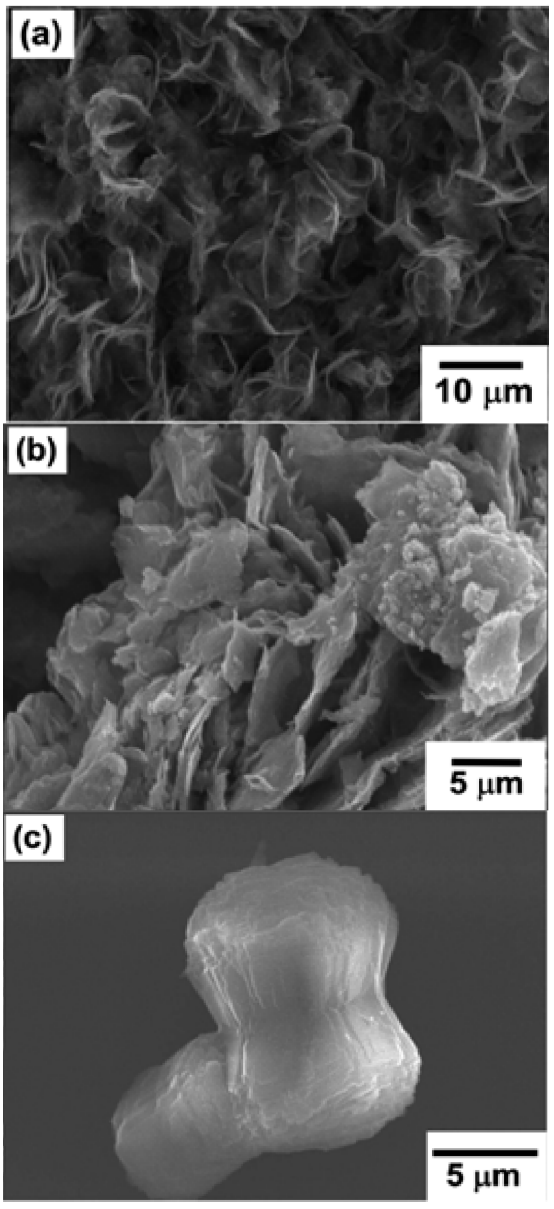

Figure 2. SEM images of (a) layered ZnO film in the absence of La^{3+} ion, (b) layered ZnO film in the presence of La^{3+} ion, and (c) layered $Zn(OH)_2$.

The lamellar structures identified in XRD pattern was also confirmed with the SEM image. In Figure 2c, layered $Zn(OH)_2$ with uniform homogeneous morphology was observed.

TEM images (Figure 3) confirmed the lamellar structures, too. Both samples had repeat distance of about 3.2 nm which had a good agreement with the values calculated from the XRD results stated above. The inset of Figure 3b depicts the electron diffraction pattern in which the host layers of layered ZnO film corresponded to the wurtzite ZnO structures. Although the intensity of the lattice spacings could not be clearly observed in the SAED pattern, the diffractions of (100), (110), and (200) could be identified. The distances of the *d*-spacings of (100), (110), and (200) were 2.83, 1.67, and 1.43 Å, respectively, which fit well with *d*-spacings of ZnO nanosheet shown in Figure 9a. Similar lamellar hybrids have

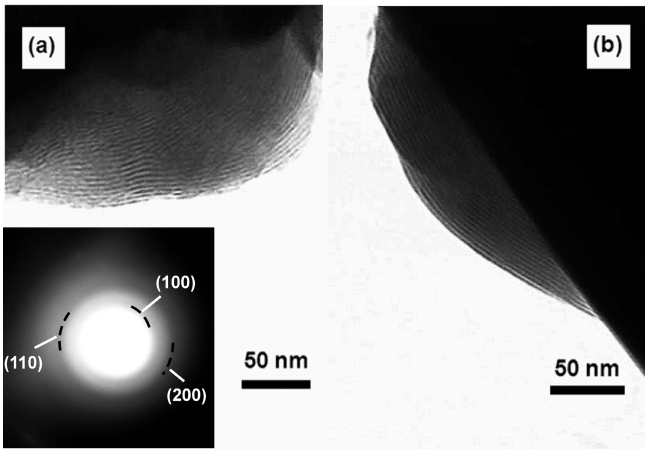

Figure 3. TEM images of (a) layered ZnO film with the SAED pattern (inset) and (b) layered $Zn(OH)_2$.

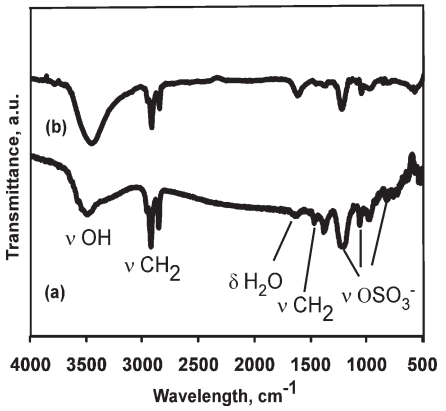

Figure 4. FTIR spectra of (a) layered ZnO film and (b) layered $Zn(OH)_2$.

been previously reported by Sofos and Goldberger et al.[36] They published lamellar ZnO hybrids having wurtzite orientation in the host layers.

In addition, UV−vis spectrum (Figure S1 in the Supporting Information) of the layered ZnO film was also performed. The absorption edge was about 380−390 nm, which was in good agreement with ZnO bandgap (about 3.2−3.3 eV), indicating that layered film is composed of ZnO. Figure S2 (Supporting Information) shows a room temperature photoluminescence spectrum for the layered ZnO films which was measured using an excitation wavelength of 330 nm. The emission band at around 385 nm was due to the near-band-edge emission of the ZnO. The wide green band emission centered at 565 nm might be caused by the oxygen vacancies or zinc interstitial defects.[28] In the light of TEM, UV−vis spectrum, and photoluminescence spectrum data of the layered ZnO films, we can conclude that the ZnO host layers formed during the electrodeposition.

In the FTIR spectra (Figure 4), the presence of stretching vibrations of alkyl chains of the surfactant ions at 2857, 2927, and 1965 cm^{-1} and the stretching modes of

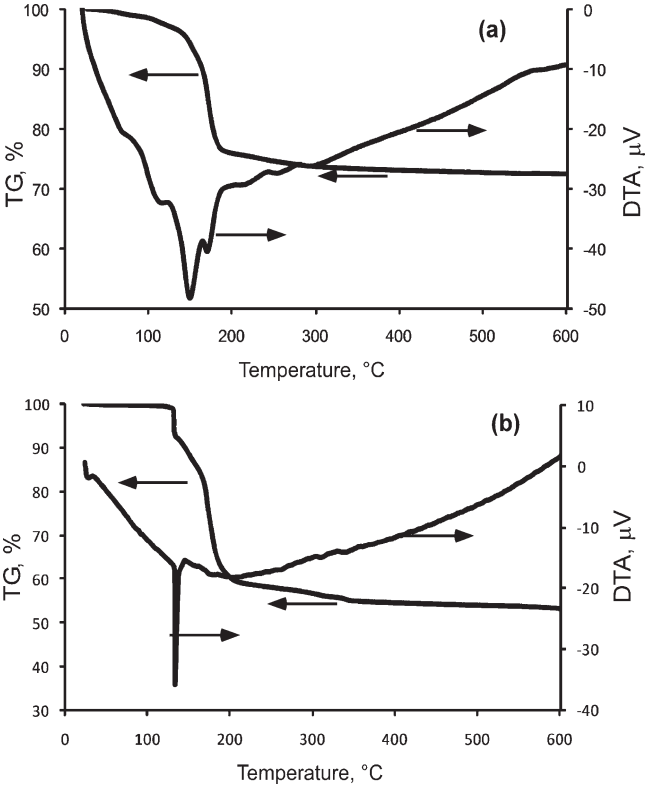

Figure 5. TG/DTA curves of (a) layered ZnO film and (b) layered $Zn(OH)_2$.

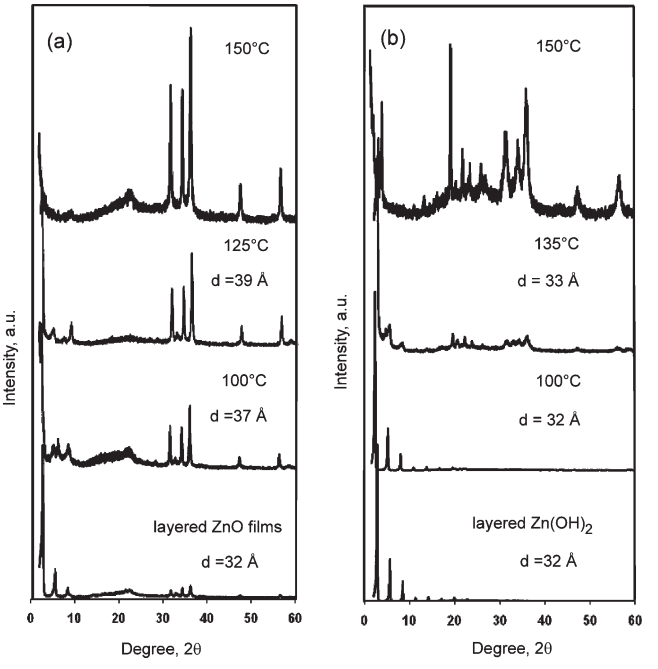

Figure 6. XRD patterns of heat treated samples of (a) layered ZnO film and (b) layered $Zn(OH)_2$.

sulfate groups in the region between 1300 and 850 cm^{-1} showed that DS^- ions intercalated between the host layers in both samples. The broad band at around 3500 cm^{-1} for ZnO layers (a) depicted the adsorption of hydroxyl groups which might be present on the surface of the ZnO hybrids. The absorption of water molecules was shown at 1677 cm^{-1} due to the δH_2O vibration for both samples.

(36) Sofos, M.; Goldberger, J.; Stone, D. A.; Allen, J. E.; Ma, Q.; Herman, D. J.; Tsai, W.-W.; Lauhon, L. J.; Stupp, S. I. *Nat. Mater.* **2009**, *8*, 68.

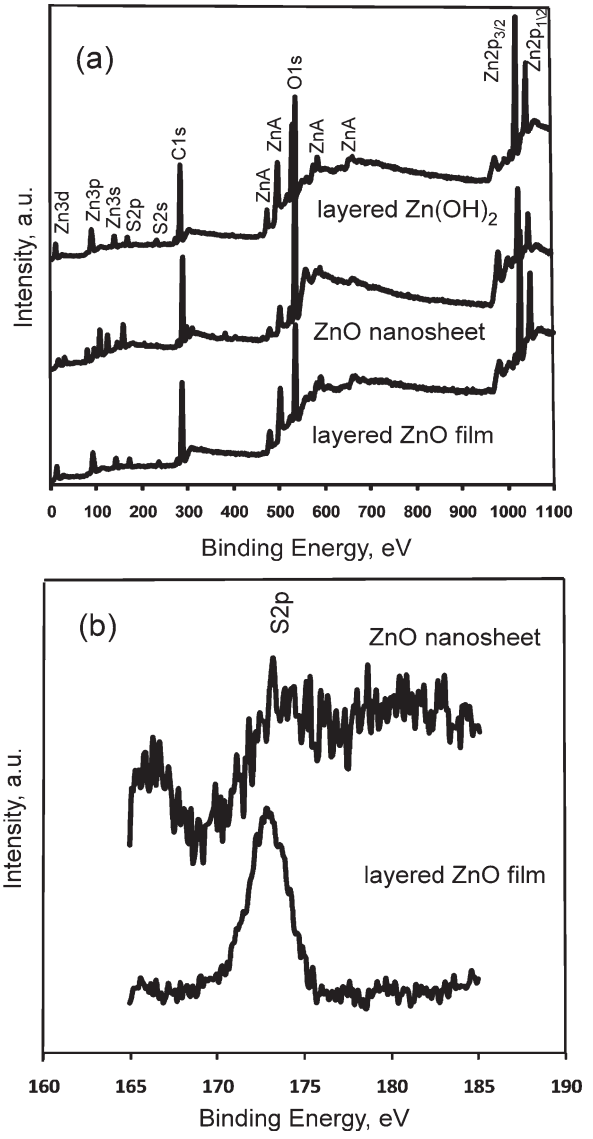

Figure 7. XPS spectra of (a) the wide scan of layered ZnO film, ZnO nanosheet on mica substrate, and layered $Zn(OH)_2$ and (b) narrow scan of S2p of layered ZnO film and ZnO nanosheet on mica substrate.

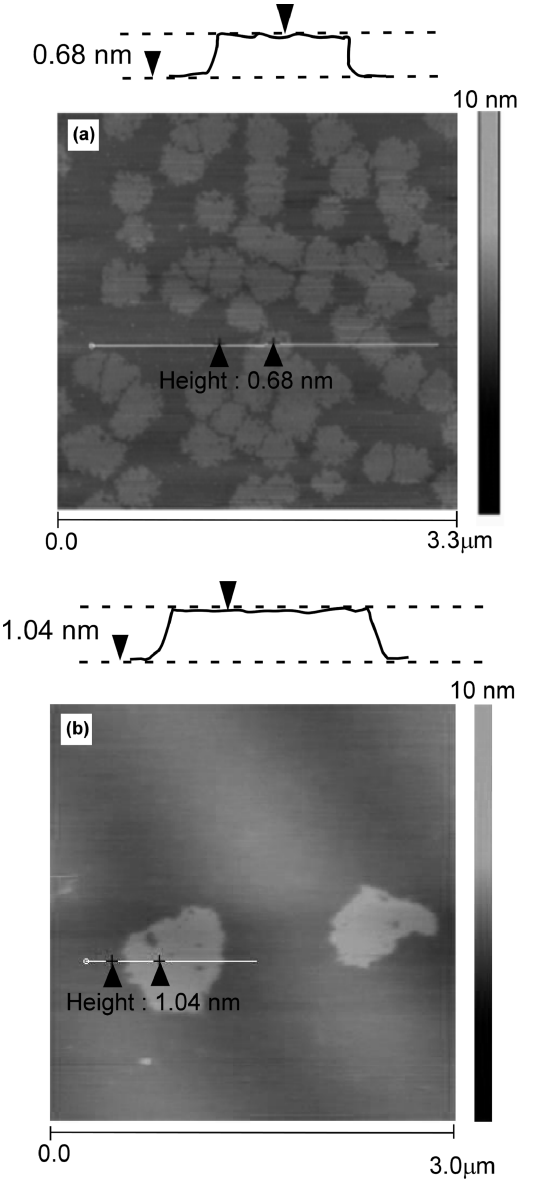

Figure 8. AFM images of (a) ZnO and (b) $Zn(OH)_2$ nanosheets.

The existence of water molecules was also confirmed by TG-DTA analysis.

Figure 5 shows the thermal behavior of the samples. The DTA signal at 114 °C for ZnO film was due to the removal of interlayer water in which the weight loss was 2%. In the case of layered $Zn(OH)_2$, if the peak at 131 °C was assumed as removal of interlayer water, the weight loss was 7.8%. According to the TG/DTA data, the chemical composition of the $Zn(OH)_{2-x}DS_x \cdot nH_2O$ was determined to be $Zn(OH)_{1.69}(DS)_{0.31} \cdot 0.78H_2O$ for layered $Zn(OH)_2$. The final product was ZnO for both samples as shown in Figure 6. However, the layered ZnO film was the mixture of layered structure and wurtzite ZnO particles as mentioned before so it might have a large error margin if we estimate the composition of the material.

The XRD patterns of heat treated samples are shown in Figure 6. Thermal stability and temperature effect on the basal spacing of both samples were studied after the heat treatment with different temperatures for 1 h. At 100 °C, the crystal structure of $Zn(OH)_2$ did not change. In contrast, the distinct difference for the crystal structure and the basal spacing were observed for the layered ZnO film, indicating it was not thermally stable compared with layered $Zn(OH)_2$. Easier collapsing of the layered structure for the layered ZnO film than the layered $Zn(OH)_2$ might occurred due to the smaller amount of DS^- ion in the layer space of the layered ZnO film, as will be stated. Since removal of interlayer water molecules were completed at 125 °C for layered ZnO film and 135 °C for layered $Zn(OH)_2$ according to the TG data, their XRD patterns were also studied at these temperatures. At 125 °C, the layered ZnO film still existed with a disordered arrangement and a further 7 Å increase occurred in the basal spacing. Heating at 135 °C of the layered $Zn(OH)_2$ resulted in the appearance of new phases in the region between 20 and 30°(2θ). Further treatment resulted in the promotion of the wurtzite ZnO phase and collapsing of the lamellar phases for both samples.

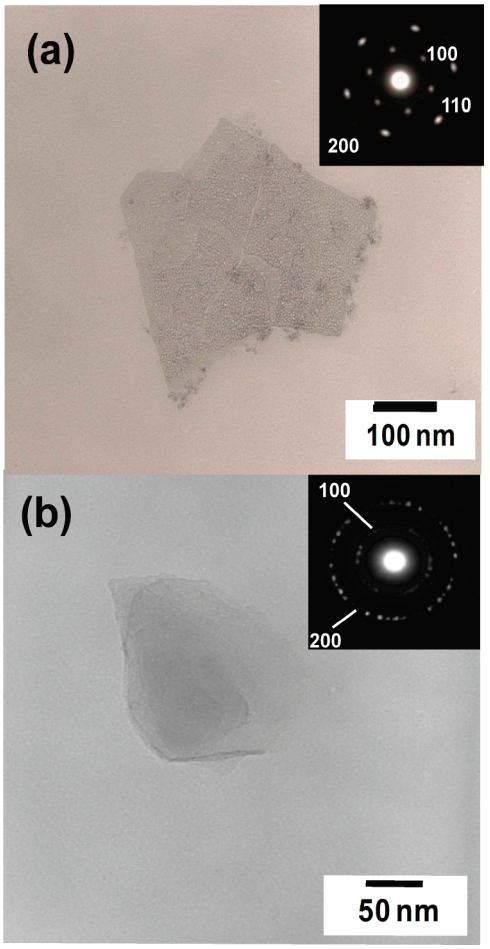

Figure 9. TEM images with SAED patterns (inset) of (a) ZnO and (b) $Zn(OH)_2$ nanosheets.

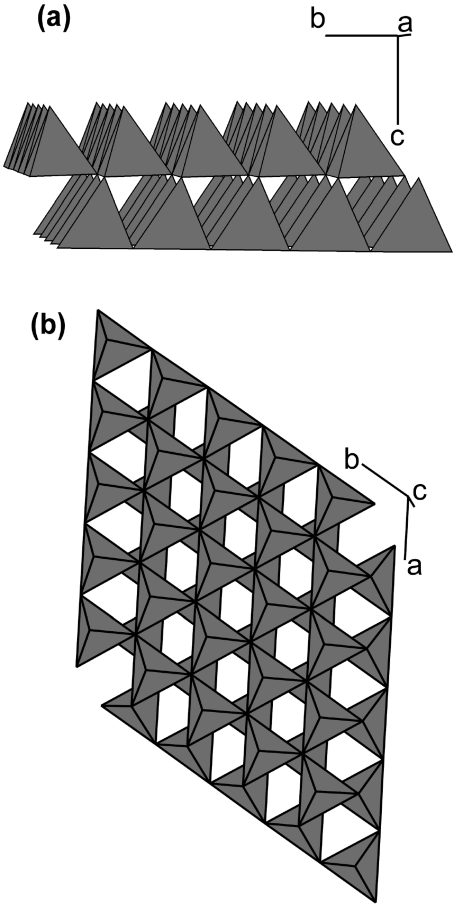

Figure 10. Structure of ZnO nanosheets: (a) side view and (b) top view.

The compositions of layered ZnO film, layered $Zn(OH)_2$, and the ZnO nanosheets were studied by XPS analyses (Figure 7). After the AFM observation, the mica substrate which had ZnO nanosheets on the surface was also analyzed by XPS technique. The wide scan of the mica showed the various peaks on the range between 20 and 200 eV as well as Zn3d, Zn3p, and Zn3s peaks. The sulfur peaks could not be identified well from Figure 7a for layered ZnO film and the ZnO nanosheet. Therefore, a narrow scan of S2p was also studied to compare the S/Zn ratio with layered ZnO film and ZnO nanosheet. The S/Zn ratio was determined 0.21 for layered ZnO film and approximately zero for ZnO nanosheet which was a good evidence for the delamination of layered ZnO film. On the other hand, the S/Zn ratio was found to be 0.51 from narrow scan of S2p (not shown) for layered $Zn(OH)_2$, indicating a smaller amount of DS^- ions in the layered ZnO film than the layered $Zn(OH)_2$. In addition, the La^{3+} ion used in the electrolyte was not included in the layered ZnO film, according to the XPS analysis.

Delamination was carried out using various solvents such as ethanol, 1-butanol, and formamide. Among them, nanosheets were obtained in 1-butanol for ZnO nanosheets. AFM images given in Figure 8a clearly shows that layered ZnO film was exfoliated into the single nanosheets. These delaminated sheets were distributed on a mica substrate homogeneously. Height analysis gave a value of 0.68 nm, which was almost in perfect agreement with the theoretical thickness of a single ZnO layer which could be 0.52 nm due to the crystal model of ZnO nanosheet, as will be stated. The delamination of the layered $Zn(OH)_2$ was successful when we used formamide rather than alcohols. Due to the height profile of $Zn(OH)_2$ nanosheets, the thickness was observed about 1 nm. The formamide can delaminate the layered structures when the highly polar carbonyl group of the formamide can make hydrogen bonds with hydroxyls part of the host layers.[37] Since ZnO film theoretically hadn't hydroxyl groups on the host layer, it might be the reason that the layered ZnO film could not be exfoliated in formamide. Moreover, delamination of the layered ZnO barely occurred when electrodeposition was carried out in the absence of La^{3+} ion. As mentioned above, the electrodeposited film consisted of layered ZnO films and a small amount of ZnO particles. The La^{3+} ion may have suppressed the formation of ZnO particles on the film so more layered ZnO films could be synthesized. On the other hand, in the absence of La^{3+} the electrodeposited films formed like aggregates with a relatively large amount of ZnO particles. We have already known that it is so much easier to delaminate the lamellar structures than the aggregates. Thus, the layered ZnO could not be

(37) Hibino, T. *Chem. Mater.* **2004**, *16*, 5482.

delaminated when electrodeposition was performed in the absence of La^{3+} ion.

TEM images with SAED patterns are shown in Figure 9. The thin nanosheet shown in Figure 9a had approximately 300 nm lateral size. The diffraction pattern recorded from the ZnO nanosheet indicated a hexagonal structure having the *d*-spacings of 2.86, 1.67, and 1.48 Å which corresponded to (100), (110), and (200) planes, respectively. The lattice constant of a_0 was estimated to be 3.3 Å from the (100) plane. According to these results, the nanosheets could attribute to the hexagonal ZnO having $a = 3.25$ Å and $c = 5.207$ Å with a space group of $P63mc$. On the other hand, the nanosheet derived from the layered $Zn(OH)_2$ had a ring-shape SAED pattern with *d*-spacings of 2.73, 1.59, and 1.38 Å with a lattice constant of 3.15 Å. Thus, these nanosheets could be β-$Zn(OH)_2$ structure[32] with lattice parameter of $a = 3.192$ Å and $c = 4.65$ Å with a space group of $P3\overline{m}1$. Eventually, the delamination of the layered materials derived from electrodeposition and soft solution processes resulted in different types of nanosheets which had wurtzite ZnO and β-$Zn(OH)_2$ orientations.

In the light of these TEM data, we considered a crystal model of ZnO nanosheets shown in Figure 10. The structure might be double layered tetrahedral coordinated oxygen atoms. The theoretical thickness of nanosheet might be 5.21 Å which is same as lattice parameter of *c* of the wurtzite ZnO. Figure 10b is the viewpoint of the nanosheets from the *c*-axis. The hexagonal structure cell fits with the diffraction pattern shown in Figure 9a.

Conclusion

In the present work, layered materials intercalated with DS^- ion were synthesized by electrochemical and soft solution processes for the preparations of ZnO and $Zn(OH)_2$ single nanosheets, respectively. The layered ZnO film was synthesized by cathodic electrodeposition process using electrolyte containing Zn^{2+}, DS^-, and La^{3+} ions at 70 °C for the preparation of ZnO nanosheets. The presence of La^{3+} ion was critical for the further delamination process. In the case of $Zn(OH)_2$ nanosheets, the layered materials were synthesized by soft solution process using the solution containing Zn^{2+}, DS^-, and HMT at 90 °C The layered ZnO film was delaminated in 1-butanol and layered $Zn(OH)_2$ was delaminated in formamide. The thicknesses of ZnO and $Zn(OH)_2$ single nanosheets were about 0.7 and 1.0 nm, respectively. According to SAED analyses, the ZnO nanosheet had wurtzite orientation while the $Zn(OH)_2$ nanosheet had β-$Zn(OH)_2$ orientation. To the best of our knowledge, this is the first report of preparation of ZnO and $Zn(OH)_2$ single nanosheets.

Acknowledgment. This work was supported by a Grant-in-Aid for Scientific Research (A) (No. 19205025) from the Japan Society for the Promotion of Science.

Supporting Information Available: UV−visible absorption spectrum and emission spectrum of layered ZnO film. This material is available free of charge via the Internet at http://pubs.acs.org.